

Quantum Monte-Carlo Studies of Generalized Many-body Systems

Jørgen Høgberget

June 17, 2013

Contents

- 1 The basics of Quantum Monte-Carlo
- 2 Live Demo
- 3 Results and Discussions

Applying the *projection operator* $\hat{\mathbf{P}}(\tau)$ on an arbitrary state $|\Psi_T\rangle$ projects the state onto the ground state of $\hat{\mathbf{H}}$ as $\tau \rightarrow \infty$.

Applying the *projection operator* $\hat{\mathbf{P}}(\tau)$ on an arbitrary state $|\Psi_T\rangle$ projects the state onto the ground state of $\hat{\mathbf{H}}$ as $\tau \rightarrow \infty$.

$$\hat{\mathbf{P}}(\tau) |\Psi_T\rangle = \exp(-(\hat{\mathbf{H}} - E_0)\tau) |\Psi_T\rangle$$

Applying the *projection operator* $\hat{\mathbf{P}}(\tau)$ on an arbitrary state $|\Psi_T\rangle$ projects the state onto the ground state of $\hat{\mathbf{H}}$ as $\tau \rightarrow \infty$.

$$\begin{aligned}\hat{\mathbf{P}}(\tau) |\Psi_T\rangle &= \exp(-(\hat{\mathbf{H}} - E_0)\tau) |\Psi_T\rangle \\ &= \exp(-(\hat{\mathbf{H}} - E_0)\tau) \sum_k C_k |\Psi_k\rangle\end{aligned}$$

Applying the *projection operator* $\hat{\mathbf{P}}(\tau)$ on an arbitrary state $|\Psi_T\rangle$ projects the state onto the ground state of $\hat{\mathbf{H}}$ as $\tau \rightarrow \infty$.

$$\begin{aligned}\hat{\mathbf{P}}(\tau) |\Psi_T\rangle &= \exp(-(\hat{\mathbf{H}} - E_0)\tau) |\Psi_T\rangle \\ &= \exp(-(\hat{\mathbf{H}} - E_0)\tau) \sum_k C_k |\Psi_k\rangle \\ &= \sum_k C_k \exp(-(E_k - E_0)\tau) |\Psi_k\rangle\end{aligned}$$

Applying the *projection operator* $\hat{\mathbf{P}}(\tau)$ on an arbitrary state $|\Psi_T\rangle$ projects the state onto the ground state of $\hat{\mathbf{H}}$ as $\tau \rightarrow \infty$.

$$\begin{aligned}\hat{\mathbf{P}}(\tau) |\Psi_T\rangle &= \exp(-(\hat{\mathbf{H}} - E_0)\tau) |\Psi_T\rangle \\ &= \exp(-(\hat{\mathbf{H}} - E_0)\tau) \sum_k C_k |\Psi_k\rangle \\ &= \sum_k C_k \exp(-(E_k - E_0)\tau) |\Psi_k\rangle \\ &= C_0 |\Psi_0\rangle + \sum_{k=1} C_k \exp(-\Delta E_k \tau) |\Psi_k\rangle,\end{aligned}$$

where $\Delta E_k > 0$ and $C_k = \langle \Psi_k | \Psi_T \rangle$.

In other words

$$\lim_{\tau \rightarrow \infty} \langle \mathbf{r} | \hat{\mathbf{P}}(\tau) | \Psi_T \rangle = \langle \Psi_0 | \Psi_T \rangle \Psi_0(\mathbf{r}). \quad (1)$$

In other words

$$\lim_{\tau \rightarrow \infty} \langle \mathbf{r} | \hat{\mathbf{P}}(\tau) | \Psi_T \rangle = \langle \Psi_0 | \Psi_T \rangle \Psi_0(\mathbf{r}). \quad (1)$$

Idea: Use an arbitrary *trial wave function* $\Psi_T(\mathbf{r})$ and perform the projection.

In other words

$$\lim_{\tau \rightarrow \infty} \langle \mathbf{r} | \hat{\mathbf{P}}(\tau) | \Psi_T \rangle = \langle \Psi_0 | \Psi_T \rangle \Psi_0(\mathbf{r}). \quad (1)$$

Idea: Use an arbitrary *trial wave function* $\Psi_T(\mathbf{r})$ and perform the projection.

Problem: Requires a priori knowledge of the exact ground state energy E_0 .

In other words

$$\lim_{\tau \rightarrow \infty} \langle \mathbf{r} | \hat{\mathbf{P}}(\tau) | \Psi_T \rangle = \langle \Psi_0 | \Psi_T \rangle \Psi_0(\mathbf{r}). \quad (1)$$

Idea: Use an arbitrary *trial wave function* $\Psi_T(\mathbf{r})$ and perform the projection.

Problem: Requires a priori knowledge of the exact ground state energy E_0 .

Solution: Introduce a *trial energy* $E_T(\tau)$. Will work as long as the trial energy drops below E_1 at a certain stage (and stays there).

In order to relate the projection process to a *Markov chain* Monte-Carlo process, τ needs to be split into sequential steps $\delta\tau$.

In order to relate the projection process to a *Markov chain* Monte-Carlo process, τ needs to be split into sequential steps $\delta\tau$.

This is achieved by using the following property of the projection operator

$$\begin{aligned}\hat{\mathbf{P}}(\tau + \delta\tau) &= \exp(-(\hat{\mathbf{H}} - E_T(\tau + \delta\tau))(\tau + \delta\tau)) \\ &= \exp(-(\hat{\mathbf{H}} - E_T(\tau + \delta\tau))\delta\tau) \\ &\quad \times \exp(-(\hat{\mathbf{H}} - E_T(\tau + \delta\tau))\tau) \\ &\simeq \exp(-(\hat{\mathbf{H}} - E_T(\tau + \delta\tau))\delta\tau)\hat{\mathbf{P}}(\tau),\end{aligned}$$

where the relation is approximate due to E_T not being constant.

Let $|\Phi(\tau)\rangle$ represent $\hat{\mathbf{P}}(\tau)|\Psi_T\rangle$. Using the relation from the previous slide reveals

Let $|\Phi(\tau)\rangle$ represent $\hat{\mathbf{P}}(\tau)|\Psi_T\rangle$. Using the relation from the previous slide reveals

$$\begin{aligned}\Phi(\mathbf{r}, \tau + \delta\tau) &= \langle \mathbf{r} | \Phi(\tau + \delta\tau) \rangle \\ &= \langle \mathbf{r} | \hat{\mathbf{P}}(\tau + \delta\tau) | \Psi_T \rangle\end{aligned}$$

Let $|\Phi(\tau)\rangle$ represent $\hat{\mathbf{P}}(\tau)|\Psi_T\rangle$. Using the relation from the previous slide reveals

$$\begin{aligned}\Phi(\mathbf{r}, \tau + \delta\tau) &= \langle \mathbf{r} | \Phi(\tau + \delta\tau) \rangle \\ &= \langle \mathbf{r} | \hat{\mathbf{P}}(\tau + \delta\tau) |\Psi_T\rangle \\ &\simeq \langle \mathbf{r} | \exp(-(\hat{\mathbf{H}} - E_T)\delta\tau) \hat{\mathbf{P}}(\tau) |\Psi_T\rangle\end{aligned}$$

Let $|\Phi(\tau)\rangle$ represent $\hat{\mathbf{P}}(\tau)|\Psi_T\rangle$. Using the relation from the previous slide reveals

$$\begin{aligned}\Phi(\mathbf{r}, \tau + \delta\tau) &= \langle \mathbf{r} | \Phi(\tau + \delta\tau) \rangle \\&= \langle \mathbf{r} | \hat{\mathbf{P}}(\tau + \delta\tau) |\Psi_T\rangle \\&\simeq \langle \mathbf{r} | \exp(-(\hat{\mathbf{H}} - E_T)\delta\tau) \hat{\mathbf{P}}(\tau) |\Psi_T\rangle \\&= \langle \mathbf{r} | \exp(-(\hat{\mathbf{H}} - E_T)\delta\tau) |\Phi(\tau)\rangle\end{aligned}$$

Let $|\Phi(\tau)\rangle$ represent $\hat{\mathbf{P}}(\tau)|\Psi_T\rangle$. Using the relation from the previous slide reveals

$$\begin{aligned}\Phi(\mathbf{r}, \tau + \delta\tau) &= \langle \mathbf{r} | \Phi(\tau + \delta\tau) \rangle \\&= \langle \mathbf{r} | \hat{\mathbf{P}}(\tau + \delta\tau) |\Psi_T\rangle \\&\simeq \langle \mathbf{r} | \exp(-(\hat{\mathbf{H}} - E_T)\delta\tau) \hat{\mathbf{P}}(\tau) |\Psi_T\rangle \\&= \langle \mathbf{r} | \exp(-(\hat{\mathbf{H}} - E_T)\delta\tau) |\Phi(\tau)\rangle \\&= \int_{\mathbf{r}'} \langle \mathbf{r} | \exp(-(\hat{\mathbf{H}} - E_T)\delta\tau) | \mathbf{r}' \rangle \Phi(\mathbf{r}', \tau) d\mathbf{r}',\end{aligned}$$

Let $|\Phi(\tau)\rangle$ represent $\hat{\mathbf{P}}(\tau)|\Psi_T\rangle$. Using the relation from the previous slide reveals

$$\begin{aligned}\Phi(\mathbf{r}, \tau + \delta\tau) &= \langle \mathbf{r} | \Phi(\tau + \delta\tau) \rangle \\&= \langle \mathbf{r} | \hat{\mathbf{P}}(\tau + \delta\tau) |\Psi_T\rangle \\&\simeq \langle \mathbf{r} | \exp(-(\hat{\mathbf{H}} - E_T)\delta\tau) \hat{\mathbf{P}}(\tau) |\Psi_T\rangle \\&= \langle \mathbf{r} | \exp(-(\hat{\mathbf{H}} - E_T)\delta\tau) |\Phi(\tau)\rangle \\&= \int_{\mathbf{r}'} \langle \mathbf{r} | \exp(-(\hat{\mathbf{H}} - E_T)\delta\tau) | \mathbf{r}' \rangle \Phi(\mathbf{r}', \tau) d\mathbf{r}',\end{aligned}$$

where $\langle \mathbf{r} | \exp(-(\hat{\mathbf{H}} - E_T)\delta\tau) | \mathbf{r}' \rangle \equiv G(\mathbf{r}', \mathbf{r}; \delta\tau)$ is a *Green's function* interpreted as the transition probability between \mathbf{r} and \mathbf{r}' .

Idea: In order to relate the Green's function to well known Markov processes, the exponential is split

$$\begin{aligned}\exp(-(\hat{\mathbf{H}} - E_T)\delta\tau) &= \exp\left(\frac{1}{2}\nabla^2\delta\tau - (\hat{\mathbf{V}} - E_T)\delta\tau\right) \\ &= \exp\left(\frac{1}{2}\nabla^2\delta\tau\right) \exp(-(\hat{\mathbf{V}} - E_T)\delta\tau) \\ &\quad + \mathcal{O}(\delta\tau^2),\end{aligned}$$

where the kinetic part describes a diffusion process with diffusion constant $D = \frac{1}{2}$, and the potential part describes a weighting (linear in position space). This is referred to as the *short time approximation*.

Problem: The Green's function has singular points in the Coulomb interaction.

Problem: The Green's function has singular points in the Coulomb interaction.

Solution: By evolving $f(\mathbf{r}, \tau) = \Phi(\mathbf{r}, \tau)\Psi_T(\mathbf{r})$ instead of $\Phi(\mathbf{r}, \tau)$ alone, the singularities are *implicitly* taken care of.

Originally:

$$\frac{\partial \Phi(\mathbf{r}, \tau)}{\partial \tau} = \left[\frac{1}{2} \nabla^2 - (\hat{\mathbf{V}} - E_T) \right] \Phi(\mathbf{r}, \tau).$$

Originally:

$$\frac{\partial \Phi(\mathbf{r}, \tau)}{\partial \tau} = \left[\frac{1}{2} \nabla^2 - (\hat{\mathbf{V}} - E_T) \right] \Phi(\mathbf{r}, \tau).$$

Importance sampled:

$$\frac{\partial f(\mathbf{r}, \tau)}{\partial \tau} = \left[\frac{1}{2} \nabla \cdot (\nabla - \mathbf{F}(\mathbf{r})) - (E_L(\mathbf{r}) - E_T) \right] f(\mathbf{r}, \tau), \quad (2)$$

where

$$\mathbf{F}(\mathbf{r}) = 2\psi_T(\mathbf{r})^{-1} \nabla \psi_T(\mathbf{r}) \quad (3)$$

is the *quantum force* and

$$E_L(\mathbf{r}) = \psi_T(\mathbf{r})^{-1} \hat{\mathbf{H}} \psi_T(\mathbf{r}) \quad (4)$$

is the *local energy*.

The Green's functions have closed form solutions on the form

$$G_{\text{Diff}}(\mathbf{r}', \mathbf{r}; \delta\tau) \propto \exp\left(-|\mathbf{r} - \mathbf{r}' - D\delta\tau\mathbf{F}(\mathbf{r})|^2 / 4D\delta\tau\right),$$

$$G_B(\mathbf{r}', \mathbf{r}; \delta\tau) \propto \exp\left(-\left(\frac{1}{2} [E_L(\mathbf{r}) + E_L(\mathbf{r}')] - E_T\right)\delta\tau\right),$$

where B denotes *branching*.

The local energy dependence in the branching Green's function implicitly takes care of the singularities in \hat{V} .

The local energy dependence in the branching Green's function implicitly takes care of the singularities in $\hat{\mathbf{V}}$.

This is done by introducing the *Jastrow factor* in $\Psi_T(\mathbf{r})$

$$J(\mathbf{r}) = \prod_{i>j}^N \exp \left(a_{ij} \frac{r_{ij}}{1 + \beta r_{ij}} \right), \quad (5)$$

where $r_{ij} = |\mathbf{r}_i - \mathbf{r}_j|$, N is the number of particles, β is a variational parameter, and a_{ij} is a constant depending on the spin eigenvalues of particles i and j .

The local energy dependence in the branching Green's function implicitly takes care of the singularities in $\hat{\mathbf{V}}$.

This is done by introducing the *Jastrow factor* in $\Psi_T(\mathbf{r})$

$$J(\mathbf{r}) = \prod_{i>j}^N \exp \left(a_{ij} \frac{r_{ij}}{1 + \beta r_{ij}} \right), \quad (5)$$

where $r_{ij} = |\mathbf{r}_i - \mathbf{r}_j|$, N is the number of particles, β is a variational parameter, and a_{ij} is a constant depending on the spin eigenvalues of particles i and j .

The Jastrow factor is tailored to cancel the singularities in the electron-electron Coulomb interaction as the relative distances decrease.

The Markov process

Idea: The process of projection is modelled by letting an ensemble of walkers span $f(\mathbf{r}, \tau)$. An iteration involves diffusing all the walkers and distributing new weights.

The Markov process

Idea: The process of projection is modelled by letting an ensemble of walkers span $f(\mathbf{r}, \tau)$. An iteration involves diffusing all the walkers and distributing new weights.

Problem: The distribution $f(\mathbf{r}, \tau) = \Phi(\mathbf{r}, \tau)\Psi_T(\mathbf{r})$ is not exclusively positive unless the nodes (zeros) of $\Psi_T(\mathbf{r})$ matches those of $\Phi(\mathbf{r}, \tau)$.

The Markov process

Idea: The process of projection is modelled by letting an ensemble of walkers span $f(\mathbf{r}, \tau)$. An iteration involves diffusing all the walkers and distributing new weights.

Problem: The distribution $f(\mathbf{r}, \tau) = \Phi(\mathbf{r}, \tau)\Psi_T(\mathbf{r})$ is not exclusively positive unless the nodes (zeros) of $\Psi_T(\mathbf{r})$ matches those of $\Phi(\mathbf{r}, \tau)$.

Solution: By *fixing* the nodes of $f(\mathbf{r}, \tau)$ to match those of $\Psi_T(\mathbf{r})$, the nodes of $\Phi(\mathbf{r}, \tau)$ will consequently match these as well. This is known as the *fixed node approximation* (FNA).

The Markov process

Idea: The process of projection is modelled by letting an ensemble of walkers span $f(\mathbf{r}, \tau)$. An iteration involves diffusing all the walkers and distributing new weights.

Problem: The distribution $f(\mathbf{r}, \tau) = \Phi(\mathbf{r}, \tau)\Psi_T(\mathbf{r})$ is not exclusively positive unless the nodes (zeros) of $\Psi_T(\mathbf{r})$ matches those of $\Phi(\mathbf{r}, \tau)$.

Solution: By *fixing* the nodes of $f(\mathbf{r}, \tau)$ to match those of $\Psi_T(\mathbf{r})$, the nodes of $\Phi(\mathbf{r}, \tau)$ will consequently match these as well. This is known as the *fixed node approximation* (FNA).

Consequence: If the FNA is not redundant, $\Phi(\mathbf{r}, \tau)$ will never converge to the exact ground state.

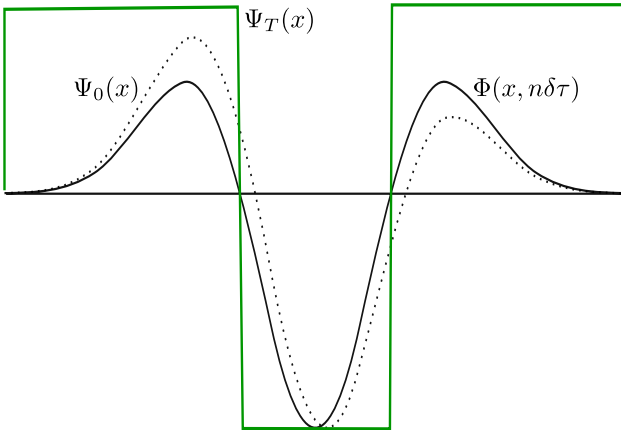


Figure: The fixed node approximation illustrated. The nodes of $\Phi(x, n\delta\tau)$ is fixed to match those of $\Psi_T(x)$.

Branching

Idea: The weights are modelled by spawning and killing walkers with a rate equal to G_B .

Branching

Idea: The weights are modelled by spawning and killing walkers with a rate equal to G_B .

Problem: G_B is not necessarily an integer.

Branching

Idea: The weights are modelled by spawning and killing walkers with a rate equal to G_B .

Problem: G_B is not necessarily an integer.

Solution: Create $\text{floor}(G_B)$ copies with a $G_B - \text{floor}(G_B)$ chance of creating an additional copy.

Branching

Idea: The weights are modelled by spawning and killing walkers with a rate equal to G_B .

Problem: G_B is not necessarily an integer.

Solution: Create $\text{floor}(G_B)$ copies with a $G_B - \text{floor}(G_B)$ chance of creating an additional copy.

Or more compact: Create

$$\bar{G}_B = \text{floor}(G_B + a) \quad (6)$$

copies, where $a \in [0, 1)$ is a uniformly distributed random number.
If the value is zero, the walker dies.

Branching

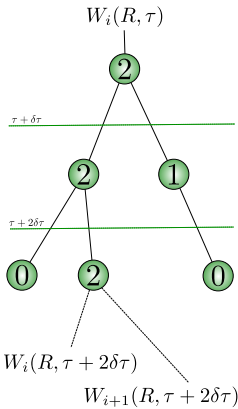


Figure: Branching illustrated. The integer values represent \bar{G}_B .

Diffusion

The diffusion equation representing G_{Diff} is the so-called *Fokker-Planck equation*.

Diffusion

The diffusion equation representing G_{Diff} is the so-called *Fokker-Planck equation*.

Anisotropic diffusion process. The quantum force pushes the walkers into regions of higher probability.

Diffusion

The diffusion equation representing G_{Diff} is the so-called *Fokker-Planck equation*.

Anisotropic diffusion process. The quantum force pushes the walkers into regions of higher probability.

According to the Fokker-Planck formalism, a new position \mathbf{r}_{i+1} is calculated from the old one, \mathbf{r}_i , as follows

$$\mathbf{r}_{i+1} = \mathbf{r}_i + D\delta\tau \mathbf{F}(\mathbf{r}_i) + \xi, \quad (7)$$

where ξ is a vector of normal distributed random numbers with variance $\sqrt{2D\delta\tau}$.

Diffusion

Problem: Due to a finite time step, the previous equations do not guarantee convergence.

Diffusion

Problem: Due to a finite time step, the previous equations do not guarantee convergence.

Solution: The *Metropolis algorithm* will correct this bias:

$$A(i \rightarrow j) = \min\{R_G(i \rightarrow j)R_\psi(i \rightarrow j)^2, 1\}, \quad (8)$$

where $i \rightarrow j$ denotes a transition from state i to state j , A is the probability of accepting the transition,

$$R_G(i \rightarrow j) = G_{\text{Diff}}(\mathbf{r}_j, \mathbf{r}_i; \delta\tau) / G_{\text{Diff}}(\mathbf{r}_i, \mathbf{r}_j; \delta\tau),$$

and

$$R_\psi(i \rightarrow j) = |\Psi_T(\mathbf{r}_j)/\Psi_T(\mathbf{r}_i)|.$$

Recap

- The projection process is approximated by the diffusion of an ensemble of walkers with distributed weights.

Recap

- The projection process is approximated by the diffusion of an ensemble of walkers with distributed weights.
- Diffusion by the Fokker-Planck equation ensures efficient sampling by the use of the quantum force.

Recap

- The projection process is approximated by the diffusion of an ensemble of walkers with distributed weights.
- Diffusion by the Fokker-Planck equation ensures efficient sampling by the use of the quantum force.
- The Metropolis algorithm corrects the bias introduced by a finite step length. Ensures that the walkers follow $|\Psi_T(\mathbf{r})|^2$.

Recap

- The projection process is approximated by the diffusion of an ensemble of walkers with distributed weights.
- Diffusion by the Fokker-Planck equation ensures efficient sampling by the use of the quantum force.
- The Metropolis algorithm corrects the bias introduced by a finite step length. Ensures that the walkers follow $|\Psi_T(\mathbf{r})|^2$.
- After each diffusion step, the walker is either killed or cloned based on the value of the branching Green's function. This ensures that the distribution of walkers follows $f(\mathbf{r}, \tau)$ and not $|\Psi_T(\mathbf{r})|^2$.

Variational Monte-Carlo

Neglecting the branching term results in a method known as *Variational Monte-Carlo* (VMC).

Variational Monte-Carlo

Neglecting the branching term results in a method known as *Variational Monte-Carlo* (VMC).

Corresponds to calculating $\langle \Psi_T | \hat{\mathbf{H}} | \Psi_T \rangle$ using a standard Monte-Carlo approach

$$\langle \Psi_T | \hat{\mathbf{H}} | \Psi_T \rangle = \int_{\mathbf{r}} |\Psi_T(\mathbf{r})|^2 E_L(\mathbf{r}) d\mathbf{r} \simeq \frac{1}{N} \sum_{i=1}^N \frac{1}{\Psi_T(\mathbf{r}_i)} \hat{\mathbf{H}} \Psi_T(\mathbf{r}_i) \quad (9)$$

Variational Monte-Carlo

Neglecting the branching term results in a method known as *Variational Monte-Carlo* (VMC).

Corresponds to calculating $\langle \Psi_T | \hat{\mathbf{H}} | \Psi_T \rangle$ using a standard Monte-Carlo approach

$$\langle \Psi_T | \hat{\mathbf{H}} | \Psi_T \rangle = \int_{\mathbf{r}} |\Psi_T(\mathbf{r})|^2 E_L(\mathbf{r}) d\mathbf{r} \simeq \frac{1}{N} \sum_{i=1}^N \frac{1}{\Psi_T(\mathbf{r}_i)} \hat{\mathbf{H}} \Psi_T(\mathbf{r}_i) \quad (9)$$

Notice that using any other distribution than $|\Psi_T(\mathbf{r})|^2$ to sample the points \mathbf{r}_i results in undefined samples of the local energy.

Variational Monte-Carlo

Variational Monte-Carlo will always result in an energy which is greater or equal to the exact ground state energy

$$\begin{aligned}\langle \Psi_T | \hat{\mathbf{H}} | \Psi_T \rangle &= \sum_{ij} C_i^* C_j \underbrace{\langle \Psi_i | \hat{\mathbf{H}} | \Psi_j \rangle}_{E_i \delta_{ij}} \\ &= \sum_i |C_i|^2 E_i \\ &= \sum_i |C_i|^2 (E_0 + \Delta E_i) \\ &= E_0 \underbrace{\sum_i |C_i|^2}_1 + \underbrace{\sum_i |C_i|^2 \Delta E_i}_{\geq 0} \\ &\geq E_0.\end{aligned}$$

The *variational principle* introduced in the previous slide opens up the possibility to introduce *variational parameters* in $\Psi_T(\mathbf{r})$ whose values are found by minimizing the VMC energy in the parameter space.

The *variational principle* introduced in the previous slide opens up the possibility to introduce *variational parameters* in $\Psi_T(\mathbf{r})$ whose values are found by minimizing the VMC energy in the parameter space.

Already have β from the Jastrow factor.

The *variational principle* introduced in the previous slide opens up the possibility to introduce *variational parameters* in $\Psi_T(\mathbf{r})$ whose values are found by minimizing the VMC energy in the parameter space.

Already have β from the Jastrow factor.

The *spatial* wave function is modelled as a single *Slater determinant*, which can be split into two parts $|\mathbf{S}(\mathbf{r})^\uparrow|$ and $|\mathbf{S}(\mathbf{r})^\downarrow|$ corresponding to two spin levels due to the fact that the Hamiltonian is assumed to be *spin independent*.

The *variational principle* introduced in the previous slide opens up the possibility to introduce *variational parameters* in $\Psi_T(\mathbf{r})$ whose values are found by minimizing the VMC energy in the parameter space.

Already have β from the Jastrow factor.

The *spatial* wave function is modelled as a single *Slater determinant*, which can be split into two parts $|\mathbf{S}(\mathbf{r})^\uparrow|$ and $|\mathbf{S}(\mathbf{r})^\downarrow|$ corresponding to two spin levels due to the fact that the Hamiltonian is assumed to be *spin independent*.

Introducing the variational parameter α into the spatial wave function yields

$$\Psi_T(\mathbf{r}; \alpha, \beta) = |\mathbf{S}(\mathbf{r}; \alpha)^\uparrow||\mathbf{S}(\mathbf{r}; \alpha)^\downarrow|J(\mathbf{r}; \beta) \quad (10)$$

Diffusion Monte-Carlo

Including both diffusion and branching results in a method known as *Diffusion Monte-Carlo* (DMC).

Diffusion Monte-Carlo

Including both diffusion and branching results in a method known as *Diffusion Monte-Carlo* (DMC).

The DMC energy corresponds to the following integral

$$E_{\text{DMC}} = \frac{\int_{\mathbf{r}} f(\mathbf{r}, \tau) \frac{1}{\Psi_T(\mathbf{r})} \hat{\mathbf{H}} \Psi_T(\mathbf{r}) d\mathbf{r}}{\int_{\mathbf{r}} f(\mathbf{r}, \tau) d\mathbf{r}} = \frac{\langle \Phi(\tau) | \hat{\mathbf{H}} | \Psi_T \rangle}{\langle \Phi(\tau) | \Psi_T \rangle}, \quad (11)$$

Diffusion Monte-Carlo

Including both diffusion and branching results in a method known as *Diffusion Monte-Carlo* (DMC).

The DMC energy corresponds to the following integral

$$E_{\text{DMC}} = \frac{\int_{\mathbf{r}} f(\mathbf{r}, \tau) \frac{1}{\Psi_T(\mathbf{r})} \hat{\mathbf{H}} \Psi_T(\mathbf{r}) d\mathbf{r}}{\int_{\mathbf{r}} f(\mathbf{r}, \tau) d\mathbf{r}} = \frac{\langle \Phi(\tau) | \hat{\mathbf{H}} | \Psi_T \rangle}{\langle \Phi(\tau) | \Psi_T \rangle}, \quad (11)$$

which upon convergence of the projection results in $\hat{\mathbf{H}} |\Phi(\tau)\rangle = E_0 |\Phi(\tau)\rangle$. The energy becomes

$$E_{\text{DMC}} = \frac{\langle \Phi(\tau) | E_0 | \Psi_T \rangle}{\langle \Phi(\tau) | \Psi_T \rangle} = E_0. \quad (12)$$

Limitations: VMC

VMC is extremely robust, however, extremely dependent on a good ansatz for $\Psi_T(\mathbf{r})$.

Limitations: VMC

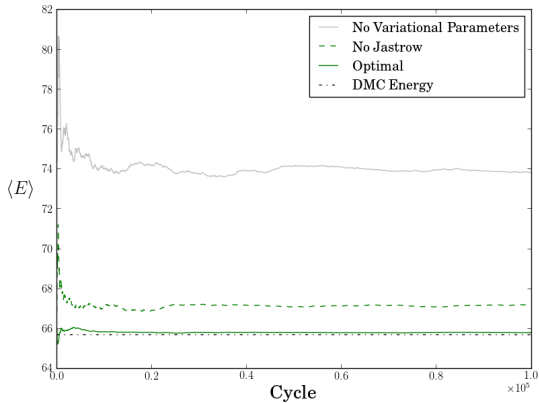


Figure: Comparison of different trial wave functions for a two-dimensional 12-particle quantum dot with unit frequency.

Limitations: DMC

As discussed previously: The fixed node approximation.

Limitations: DMC

As discussed previously: The fixed node approximation.

Problem: The branching can get out of control for high *variance* systems.

Limitations: DMC

As discussed previously: The fixed node approximation.

Problem: The branching can get out of control for high *variance* systems.

Solution: Can be countered by choosing a lower time step.

Limitations: DMC

As discussed previously: The fixed node approximation.

Problem: The branching can get out of control for high *variance* systems.

Solution: Can be countered by choosing a lower time step.

Consequence: Slower convergence. Breaking the requirement of *ergodicity*.

Limitations: DMC

Diffusion Monte-Carlo is not as dependent on the trial wave function as VMC.

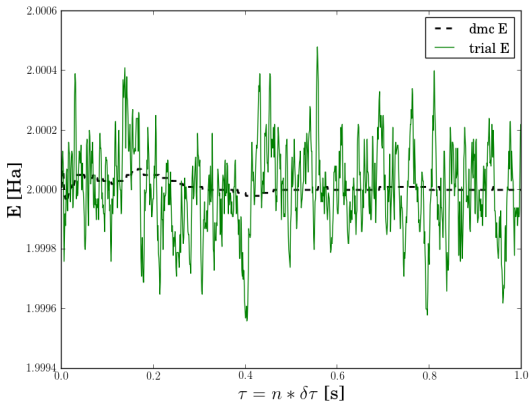


Figure: DMC calculation without the exact wave function. The exact result is $E_0 = 2$. The VMC energy is $2.0042(3)$, whereas the DMC energy is $2.00000(2)$.

Beskriv og vis minimering av trial wave function real time. Beskriv og vis VMC + blockingprosessen real-time. Vis VMC qdots 2d vmc og DMC real time konvergens. vis skalering showoff distribusjoner?

ω	E _{VMC}	E _{DMC}	E _{FCI}
0.01	0.07406(5)	0.073839(2)	0.07383505
0.1	0.44130(5)	0.44079(1)	0.44079191
0.28	1.02215(5)	1.02164(1)	1.0216441
0.5	1.66021(5)	1.65977(1)	1.6597723
1.0	3.00030(5)	3.00000(1)	3.0000001

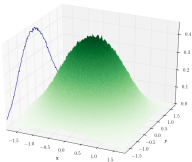
Figure: Two-particle results for two-dimensional quantum dots compared with FCI results by Veronica K.B. Olsen.

N	ω	E _{VMC}	E _{DMC}	E _{SRG}	E _{CCSD}
42	0.1	107.881(1)	107.6389(2)	-	111.7170 {8}
	0.28	220.161(1)	219.8426(2)	219.8836 {14}	222.1401 {8}
	0.5	331.002(1)	330.6306(2)	330.6485 {14}	331.8901 {8}
	1.0	544.2(8)	542.9428(8)	542.9528 {14}	543.1155 {18}
56	0.1	176.269(2)	175.9553(7)	-	186.1034 {9}
	0.28	358.594(2)	358.145(2)	-	363.2048 {9}
	0.5	538.5(6)	537.353(2)	-	540.3430 {9}
	1	880.2(7)	879.3986(6)	-	879.6386 {17}

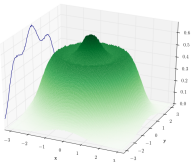
Figure: Results for two-dimensional quantum dots 42 and 56 particles compared with SRG results by Sarah Reimann and CCSD results by Christoffer Hirth.

N	ω	E _{VMC}	E _{DMC}	E ₀
2	0.01	0.07939(3)	0.079206(3)	-
	0.1	0.50024(8)	0.499997(3)	0.5
	0.28	1.20173(5)	1.201725(2)	-
	0.5	2.000005(2)	2.000000(2)	2.0
	1.0	3.73032(8)	3.730123(3)	-
8	0.1	5.7130(6)	5.7028(1)	-
	0.28	12.2040(8)	12.1927(1)	-
	0.5	18.9750(7)	18.9611(1)	-
	1.0	32.6842(8)	32.6680(1)	-
20	0.1	27.316(2)	27.2717(2)	-
	0.28	56.440(2)	56.3868(2)	-
	0.5	85.714(2)	85.6555(2)	-
	1.0	142.951(2)	142.8875(2)	-

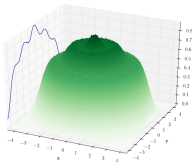
Figure: Results for three-dimensional quantum dots compared with exact solutions by M. Taut.



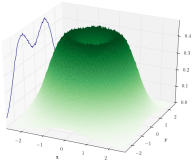
$N = 2$



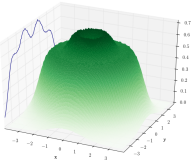
$N = 12$



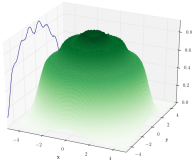
$N = 30$



$N = 6$



$N = 20$



$N = 42$

Figure: DMC one-body densities for two-dimensional quantum dots.

VMC density $|\Psi_T(\mathbf{r})|^2$

DMC density $\Phi(\mathbf{r}, \tau)\Psi_T(\mathbf{r})$

Pure density $|\Phi(\mathbf{r}, \tau)|^2$

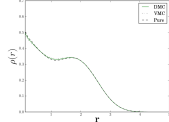
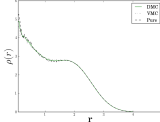
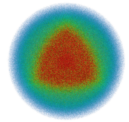
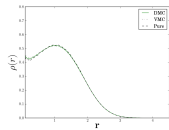
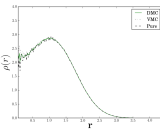
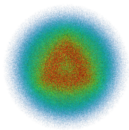
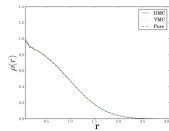
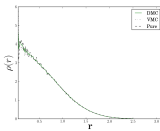
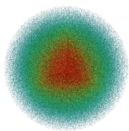


Figure: One-body densities for two- and three-dimensional quantum dots.

Lowering the frequency

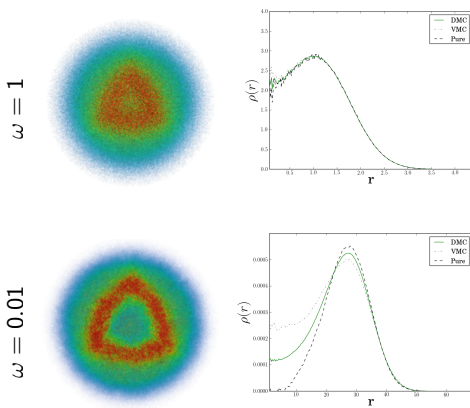
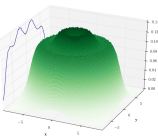
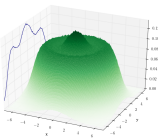
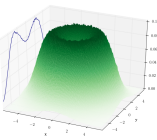
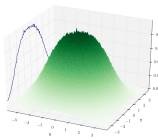
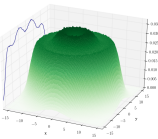
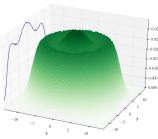
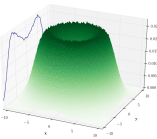
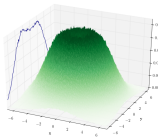


Figure: One-body densities for a 8-particle three-dimensional quantum dot for high and low frequencies.

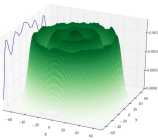
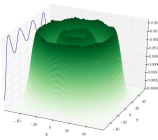
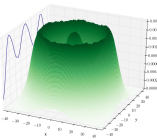
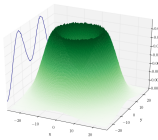
$\omega = 0.28$



$\omega = 0.1$



$\omega = 0.01$



$N = 2$

$N = 6$

$N = 12$

$N = 20$

